Available online at www.sciencedirect.com
ScienceDirect
Journal of the European Ceramic Society 27 (2007) 3439–3444
www.elsevier.com/locate/jeurceramsoc

Characterisation of the *R–T* response of $BaTiO_3$ thermistors on three different length scales

L. Affleck, J. Seaton [1], C. Leach [*]

Materials Science Centre, University of Manchester, Grosvenor Street, Manchester M1 7HS, UK

Received 30 April 2005; received in revised form 19 May 2006; accepted 26 May 2006
Available online 9 April 2007

Abstract

Scatter in the resistance–temperature (*R–T*) characteristic of $BaTiO_3$-based PTC thermistors was investigated on three scales of measurement, corresponding to bulk pellet, a region approximately six grains wide, and single grain boundaries. On the bulk pellet scale the *R–T* responses were highly consistent with only small variations in peak resistance. Comparison of *R–T* measurements across pairs of electrodes separated by approximately six grain diameters revealed systematic changes with position across the pellet, as well as local scatter, corresponding to local resistivity differences of up to a factor of five on the 50 μm scale in the PTC region. These were attributed to differences both in local composition and the local level of porosity, which affects oxidation during cooling. The *R–T* responses of individual high angle grain boundaries showed significant variations in PTC curve shape and degree of field dependence between boundaries.

Keywords: Electrical properties; PTC devices; Grain boundaries; Local properties; $BaTiO_3$

1. Introduction

Positive temperature coefficient of resistance (PTC) thermistors show a large increase in resistance over a small temperature interval, just above the Curie temperature, T_C, which for devices based on $BaTiO_3$ is about 130 °C. The increase in resistance, of several orders of magnitude, is associated with a ferroelectric to paraelectric phase transformation and the development of resistive barriers at the grain boundaries.[1,2]

The shape of the PTC curve can be affected by a number of physical factors including sintering atmosphere, cooling rate, grain size, porosity, and the type, amount and distribution of dopants. Donor dopants such as Y^{3+} or La^{3+} are added to provide n-type semiconductivity.[2–4] Acceptors such as Mn increase the height of the grain boundary barrier by activating deep trap states.[4–7] Isovalent substitutions of Pb or Sr for Ba are used to adjust T_C[8] or are added in 'balancing' amounts to modify performance whilst maintaining T_C.[9] Ca has little influence on T_C, but is often also added as a grain refiner.[10] Sintering aids such as SiO_2 are commonly used both to achieve a uniform distribution of dopants and to improve densification through liquid phase sintering.[3,6]

Commercial demands require close tolerance of pellet performances within a batch, and to this end great care is taken to ensure homogeneous mixing of the starting materials. However, subsequent processing, and especially the sintering process, can amplify small density and compositional fluctuations within the pellets. Consequently, as the scale of measurement is reduced down to the single grain boundary level many workers have reported that spatial variations occur in the PTC response.[11–14] This is undesirable from a materials quality viewpoint, where any inhomogeneity of electrical behaviour is likely to increase transient stresses during switching when high levels of power are being dissipated, possibly leading to premature device failure.

Kuwabara et al.[11] performed measurements across single grain boundaries using specially prepared bicrystals of PTC thermistor. Normal and saw-tooth shaped PTC curves were observed, as well as grain boundaries that showed no significant PTC effect. The reason for these different behaviours was not established, although the authors suggested that the influence of acceptor traps and grain boundary morphology may be significant. Nemoto and Oda[12] measured the electrical characteristics of individual grain boundaries in barium titanate PTC ceramics

* Corresponding author. Tel.: +44 161 306 3561; fax: +44 161 306 3586.
E-mail address: colin.leach@manchester.ac.uk (C. Leach).
1 Present address: GE Infrastructure Sensing, Taunton, UK.

0955-2219/$ – see front matter © 2006 Elsevier Ltd. All rights reserved.
doi:10.1016/j.jeurceramsoc.2006.05.096

with 100 μm diameter grains. They noted a large variation in the PTC magnitude, of at least two orders of magnitude, and slight variations in T_C between boundaries, which they related to variations, both in trap density and the thickness of an intergranular layer. Hayashi et al.[13,14] studied grain boundaries in bicrystals, and individual grain boundaries in 1 mm grain size material. They found that many low angle and low Σ coincidence site lattice (CSL) boundaries did not show a PTC effect, whereas, random high angle boundaries did—although the PTC magnitude of the random boundaries did vary. They suggested that this might be due to the effect of differences in oxygen diffusivity between boundaries that changed the extent of grain boundary reoxidation during sintering.

Hayashi et al.[15] also investigated the influence of grain boundary plane on the PTC response by cutting curved grain boundaries in coarse-grained Nb-doped $BaTiO_3$ into segments; each segment had the same misorientation, but the grain boundary planes differed. They found that, in general, the PTC magnitude increased with increasing tilt angle of the grain boundary plane.

The studies reviewed in the previous paragraph are all based around specially prepared, coarse-grained materials or bicrystals, which may show characteristics that differ from those of grain boundaries in commercial fine-grained devices. It is currently unclear whether such a broad spectrum of properties is generally observed in real devices where less grain growth has occurred. The purpose of our investigation was to address this question by investigating the homogeneity of the electrical behaviour of fine-grained PTC thermistors. This was achieved by comparing the consistency of *R–T* response with the scale on which it is measured, from bulk pellet, across a few grains, to individual grain boundaries.

2. Experimental

Electrical and microstructural characterisations were made on thermistors prepared from a proprietary powder mix (GE Infrastructure, MIX096) based on co-doped $BaTiO_3$ with additions of Ca, Pb and Sr; a ‘so-called’ SPC composition. Thermistor compacts were sintered in muffle furnaces in an air atmosphere at peak temperatures of 1300 and 1400 °C, with heating and cooling rates of 80–130 $°C\,h^{-1}$, yielding pellets 8 mm in diameter and 2 mm thick.

Electrical measurements of resistance versus temperature (*R–T*) were performed using a Keithley 487 picoammeter, computer controlled to measure the resistance at a range of applied biases and temperatures. Microstructures were studied using a Philips XL30 FEG-SEM. Grain boundary misorientations were determined by electron backscattered diffraction pattern (EBSP) analysis, using a Philips XL30 FEG-SEM with HKL Channel+ software.[16,17]

Measurements were made on three scales: (1) *bulk* pellet; (2) 25 μm scale corresponding to about six grain diameters (termed *mesoscale*); (3) individual grain boundaries (termed *microscale*).

For the bulk pellet *R–T* measurements, ohmic Ti electrodes were deposited by sputtering onto both pellet faces. Measurements were made at an applied bias equivalent to 0.1 V/grain boundary to allow direct comparison of bulk with mesoscale and microscale data.

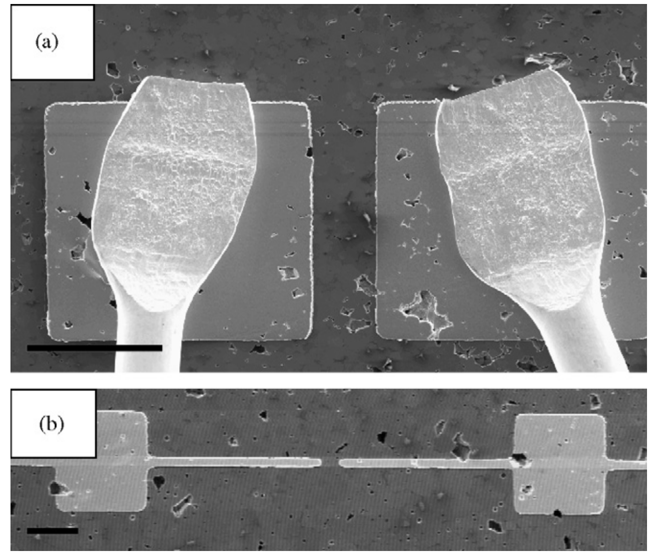

Fig. 1. Surface mounted pads used for (a) mesoscale and (b) microscale *R–T* measurements (scale bars = 50 μm).

Photolithographic and sputtering techniques were used to deposit ohmic Ti electrodes onto a polished cross-section of the thermistor for the mesoscale and microscale measurements. In the case of the mesoscale measurements, the electrodes were in the form of 100 μm squares, separated by 25 μm (Fig. 1a). For the microscale measurements pairs of electrodes comprising 100 μm squares, each with 200 μm long, 10 μm wide arms were deposited (Fig. 1b). The separation between the ends of the electrode arms was about 20 μm. The extended shape of the electrodes was chosen so that the majority of the current would flow between the ends of the electrode arms rather than between the square pads. Electrode pairs where a single grain boundary was found to lie within the gap were selected for study. Connections were made to the electrode pads by microbonding with 25 μm diameter gold wires. In each case, an applied bias corresponding to 0.1 V/grain boundary was used. For field dependency measurements, voltage biases in the range 0.1 to 1 V/grain boundary were used.

3. Results and discussion

The pellets sintered at 1300 °C had a mean grain size of 4 μm and a density 93% of theoretical, whilst the pellets sintered at 1400 °C had a mean grain size of 20 μm and a density of 92%.

3.1. Bulk pellet measurements

Comparative *R–T* curves, collected from pellets sintered at 1300 and 1400 °C, measured at fields corresponding to 0.1 V/grain boundary are shown in Fig. 2a and b, respectively. The PTC magnitude, defined as $\log(R_{max}/R_{min})$, where R_{max} is the peak resistance and R_{min} is the minimum measured value, normally occurring just below T_C, is about 5 in the pellets that

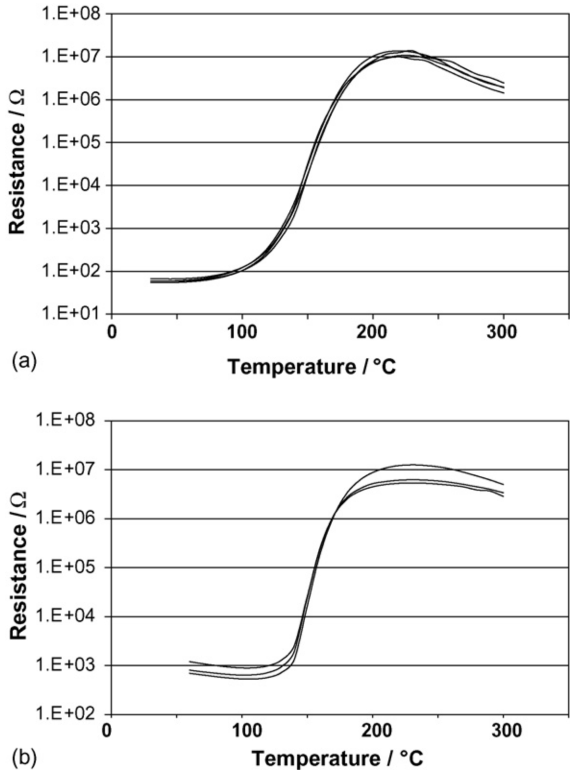

Fig. 2. *R–T* characteristics of pellets sintered at (a) 1300 °C and (b) 1400 °C.

were sintered at 1300 °C, and about 4 for pellets that were sintered at 1400 °C. The reproducibility of *R–T* characteristic between the pellets sintered at 1300 °C is very good (Fig. 2a), with similar curve shapes. The greatest variability between curves occurs in the high temperature negative temperature coefficient of resistance (NTC) region, and is associated with slight variations in R_{max}. However, the responses of the pellets sintered at 1400 °C are much less consistent (Fig. 2b); there is a wider distribution of R_{min} values, together with significant differences in R_{max}. There are also slight variations in the gradients of the PTC slopes.

On this scale of measurement, it would be expected that differences in the performance of individual grain boundaries would average out through the bulk pellet on account of the sheer numbers involved. However, the high level of scatter in the bulk pellet characteristics observed in the 1400 °C samples is unexpected, reflecting poor consistency of performance between pellets.

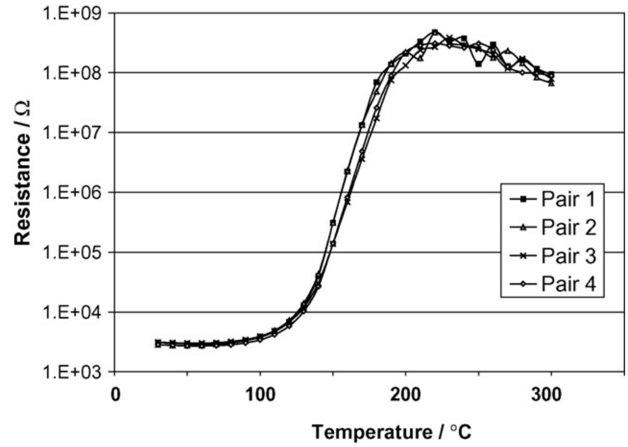

Fig. 4. *R–T* plots for each of the pad pairs 1–4, shown in Fig. 3.

3.2. Mesoscale measurements

R–T measurements were made between pairs of surface mounted electrodes, separated by approximately six-grain diameters, at various locations on the polished face of a 1300 °C sintered thermistor pellet, using an applied field of 0.1 V/grain boundary. The uniformity of electrical behaviour was investigated by comparing a series of *R–T* curves that were collected within the central region of the pellet, using four electrode pad pairs, located within 500 μm of each other (Fig. 3). The *R–T* curves for each of these electrode pairs are shown in Fig. 4. Comparison of the bulk pellet (Fig. 2a) and mesoscale (Fig. 4) *R–T* characteristics shows that they yield almost identical curves with a similar PTC magnitude and PTC gradient, although the differences in electrode geometry mean that the absolute values of resistance differ. This similarity in the shapes of the curves collected using these two electrode configurations suggests that

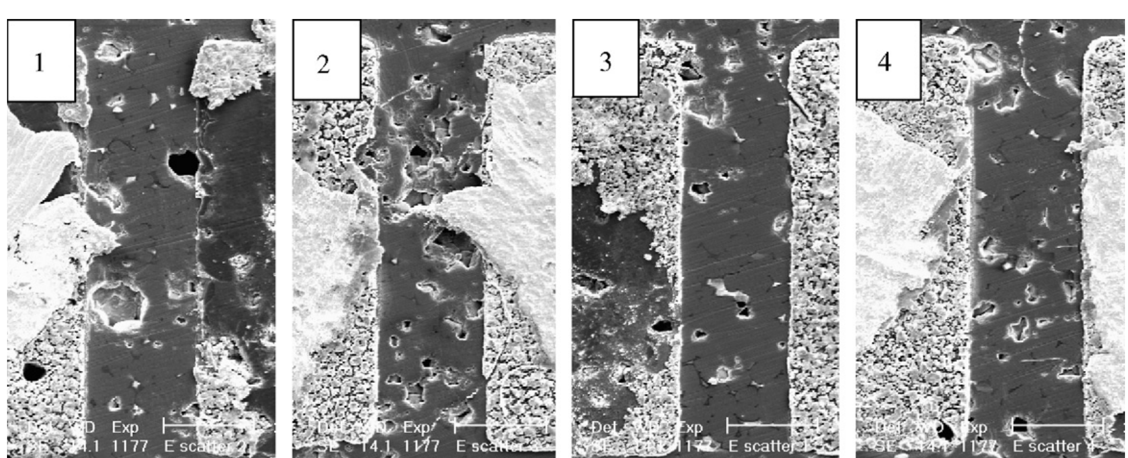

Fig. 3. Inter-electrode regions of pad pairs 1–4, from the central region of the pellet (scale bar = 20 μm).

the mesoscale measurement do indeed reflect the localised 'bulk' properties without being affected by factors such as enhanced surface diffusion, and validates the use of surface mounted electrodes for making localised *R–T* measurements that are directly comparable with bulk data.

Whilst the T_C, R_{min} and R_{max} values for each of the local *R–T* curves are consistent, there are small differences in the gradients of the PTC curves. These may be quantified by expressing the PTC gradient as $\log(R_{160}/R_{120})$, where R_{160} and R_{120} are the measured resistances at 160 and 120 °C, respectively. On this basis the gradient for electrode pairs 1 + 2 is 2.5, whereas, for pairs 3 + 4 it is 2.0.

Ting et al.[4] observed an increase in $\log(R_{160}/R_{120})$ from 1 to 2 as the Mn content was increased from 0 to 0.02 mol%. Illingsworth et al.[7] observed a similar increase from 2.3 to 2.5 as the Mn content was raised from 0 to 0.04 at.%. Thus the observed differences in our samples could be explained by localised small changes in Mn concentration due, for example, to incomplete mixing on this scale during powder preparation. However, since this would also have the effect of producing large changes in R_{max} and R_{min}, which we do not observe in our study, it is unlikely that this is the reason. Small differences in donor doping levels are also reported to affect the PTC magnitude[18] but there is no reported evidence that the gradient of the curve is also modified.

Another possible explanation is microstructural. There is a greater number of large pores between electrode pairs 1 + 2 than between pairs 3 + 4 (Fig. 3). This increased porosity is associated with a steeper PTC curve. Oxidation at the grain boundaries during cooling is essential for maximising the PTC effect, because it creates surface acceptor states that increase barrier height.[19] For example, Ueoka and Yodogawa[6] observed a steepening of the (bulk) PTC slope in their samples due to enhanced grain boundary oxidation as the oxygen content of the sintering atmosphere was increased from 0.5 to 20% oxygen. The thermistors prepared for this study have a density of 92–93% with porosity lying predominantly at the grain boundaries, suggesting that much of this porosity is open. This open porosity will allow oxygen to permeate deep into the ceramic, increasing the oxidation of grain boundaries in the vicinity of the pores. The higher levels of porosity visible in areas 1 and 2 may therefore be suggestive of greater grain boundary oxidation, compared with areas 3 and 4, which appear further from the pore network, and therefore of a steeper *R–T* curve.

These local differences in the gradients of the *R–T* curves mean that, at intermediate temperatures, say around 160 °C, variations of up to five times in resistivity can exist within the sample on the 25 μm scale, leading to similar differences in the local current density.

In a previous study[20] of this material a steady decrease in T_C of up to 12 °C was observed in the outer 300 μm of the sintered thermistor pellet. It was shown that this arose from Pb loss during sintering and that the affected region accounted for about 20% of the pellet volume. In the context of this work, we can now consider the combined effects of this systematic change in T_C and the local variations in PTC slope on the overall response of the thermistor.

As the thermistor is heated, the Pb depleted outer region of the pellet will initially pass through T_C and begin to enter a high resistance state, whilst the core of the pellet remains below T_C. Since the core and surface regions of the pellet are effectively connected in series between the electrodes, any current passing between the electrodes must pass both through these volumes. Until the core of the pellet reaches T_C, the resistance increase of the bulk device is exclusively due to the increase in the near surface region. However, as the temperature is increased further the pellet core also passes through T_C and enters the PTC region and, due to it occupying the larger volume fraction of the pellet, rapidly dominates the overall PTC behaviour. Thus the Pb concentration gradient means that the initial response within the PTC region is smeared out, resulting in a broadening of the overall pellet's *R–T* curve just above R_{min}, relative to a homogeneous pellet, and reducing the initial PTC gradient. Local variations in the PTC gradient will mean that there are fine-scale differences in sample resistivity that will result in preferred current pathways through the sample as the current is channelled around higher resistance regions. This behaviour will not affect the bulk *R–T* curve shape significantly, since the local field is not increased. However, it may result in a transient build-up of local stress at the interfaces between high and low resistance regions during rapid switching, particularly when caused by Joule heating at high current densities.

3.3. Microscale measurements

Fine-scale *R–T* measurements were made on a sample sintered at 1400 °C, using the electrode configuration shown in Fig. 1b. The gap between the ends of the electrode arms was 20 μm. In cases where both electrode arms terminated in the same grain, the *R–T* characteristic showed a flat response (Fig. 5a), consistent with the inter-electrode current passing between the ends of the electrode arms. When a single grain boundary lay between the electrodes it was considered that most of the current would pass through this grain boundary, as it would offer the lowest resistance pathway between the electrodes (other routes would require two or more grain boundaries to be traversed). For the measurements the applied field was 0.1 V/grain boundary.

R–T measurements were made across four single grain boundaries (Fig. 5b). The misorientations of each of the grain boundaries were calculated from EBSP data: all were classified as random high angle, i.e. no grain boundary was indexable with $\Sigma < 50$. Each grain boundary reproducibly exhibited a large PTC magnitude, with $\log(R_{max}/R_{min})$ in the range 3.5–3.8. This value was consistent with the PTC magnitude of the pellets sintered at 1400 °C. A small variation in R_{min} (<5%) was observed between the grain boundaries.

The gradients of the PTC curves for grain boundaries 1 and 2 change noticeably with temperature: above 170 °C they reduce by 30% relative to the curves for grain boundaries 3 and 4, which show a more uniform gradient over the PTC range. Jonker[2] and Kuwabara[21] noted similarly shaped curves, with an initial steep gradient near T_C followed by a reduction at higher temperatures. This change in slope was attributed to a changeover

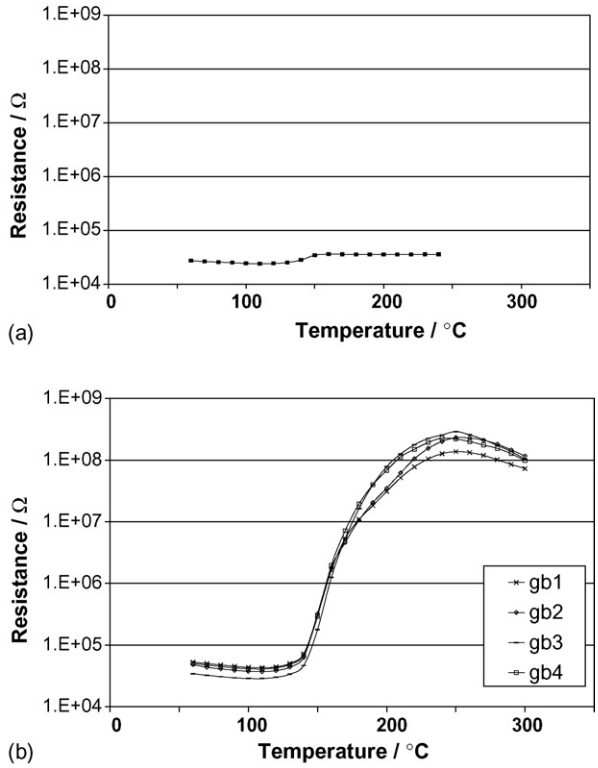

Fig. 5. (a) The R–T response within a single grain. (b) The R–T responses of four different grain boundaries.

between the processes giving rise to the initial jump in resistance just above T_C and the ferroelectric compensation at higher temperatures.[2] In our samples, we have observed individual grain boundaries where the balance of these processes differs, resulting in differences in PTC behaviour between grain boundaries. In all four-grain boundaries T_{max} is consistently in the range 240–250 °C indicating similar acceptor trap depths at all grain boundaries.

The influence of an applied electric field on the grain boundary barrier height was studied over a voltage range of 0.1–1 V/grain boundary. Two types of behaviour were observed, corresponding to strong and weak field dependence. An R–T plot for a strongly field dependent grain boundary is shown in Fig. 6 and that for a weakly field dependent grain boundary in Fig. 7.

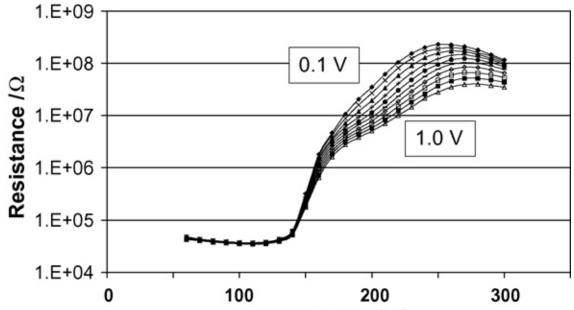

Fig. 6. R–T plot of gb2 as a function of applied voltage from 0.1 to 1.0 V. The grain boundary shows a strong field dependence.

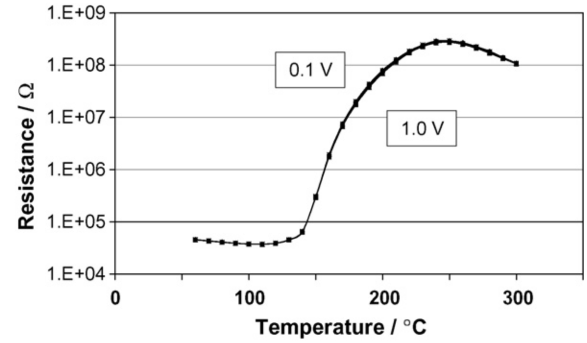

Fig. 7. R–T plot of gb4 as a function of applied voltage from 0.1 to 1.0 V. The grain boundary shows a weak field dependence.

The field dependence of the resistance of a PTC thermistor above T_C is indicative of the grain boundary barrier structure and hence the conduction mechanism. There are several published models describing the nature of the barrier structure in PTC thermistors.[22] Generally, different models predict different field dependences of resistance, and so fitting the field dependence is a good way to test the validity of these models. Although none of the data collected in this study fitted the predictions of any of the common models over an extended voltage range, when our R–T data was plotted as I versus V^2, as a test for the space charge limited current (SCLC) model, a significant difference was observed between the strongly and weakly field dependent boundaries (Fig. 8). Whilst at low fields (<0.05 V/grain boundary) the grain boundaries do show a $I = kV^n$ relationship where $n = 2$, as given by the dotted line, as the applied field increases the high and low field dependent grain boundary plots diverge from the SCLC gradient in opposite ways. The strongly field dependent boundaries have $n > 2$, whereas, those boundaries with a weak field dependence had $n < 2$. This variation demonstrates that there are differences in grain boundary electrical structure between grain boundaries, and questions the use of bulk pellet data in attempting to fit field dependence data to proposed conduction models.

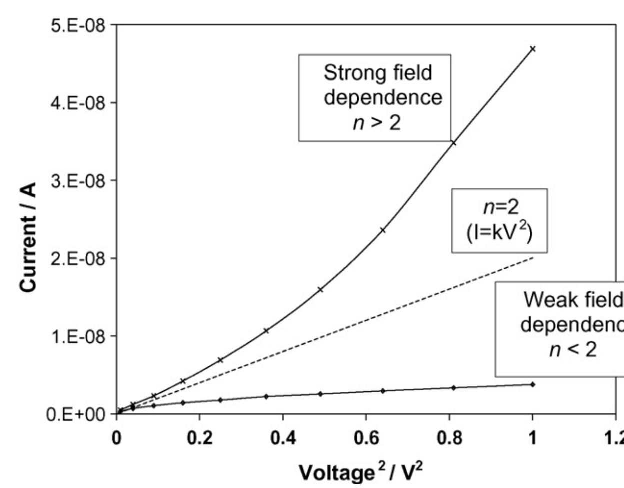

Fig. 8. I–V^2 plot for grain boundaries showing strong and weak field dependencies.

In contrast, mesoscale measurements of field dependency at fields in the range 0.2–1 V/grain boundary showed only a relatively strong dependency. This may be readily explained, since with an electrode spacing of, typically, six grain diameters there are many different current pathways that can be followed through different sets of interfaces. Those boundaries that are strongly field dependent will provide lower resistance pathways when a field is applied, and will channel the current flow preferentially. However, it is unlikely that a complete pathway will exist through strongly field dependent grain boundaries between the electrodes and so the overall field dependence between these widely spaced electrodes will be somewhat less than that of a single highly field dependent grain boundary. This is borne out experimentally since, as the field is increased from 0.2 to 1 V/grain boundary, the PTC magnitude decreases by ~6% on the mesoscale, whereas, on the microscale it decreases by ~2% for a single weakly and by ~18% for a single strongly field dependent grain boundary.

4. Summary

Differences in the *R–T* response of PTC thermistor material are observed to change with the scale of measurement. Bulk pellets showed reproducible behaviour with only slight scatter. On the mesoscale, systematic changes in *R–T* behaviour with distance, as well as local scatter were observed. On the microscale, larger differences in the PTC slope and magnitude were observed due to the reduced effect of averaging of properties.

Grain boundaries in PTC thermistors show different electrical structures, which are manifested through differences in field dependence of resistance. Individual grain boundaries could show either a weak or a strong field dependence. These differences may be caused by variations in the physical and electrical structure of the grain boundary regions, due to differences in crystallographic mismatch, doping or defect concentrations. More detailed measurements are currently being made to characterise the range of field dependencies that are observed.

The inhomogeneities in the *R–T* response have implications for thermistor performance and may lead to increased mechanical stress under electrical loading.

Acknowledgements

This work was funded through EPSRC grant number GR/R00500/01. GE Infrastructure Sensing is thanked for the supply of the thermistor pellets used in this study.

References

1. Heywang, W., Resistivity anomaly in doped barium titanate. *J. Am. Ceram. Soc.*, 1964, **47**, 484–490.
2. Jonker, G. H., Some aspects of semiconducting barium titanate. *Solid-State Electron.*, 1964, **7**, 895–903.
3. Fagan, J. G. and Amarakoon, V. R. W., Reliability and reproducibility of ceramic sensors. Part II. PTC thermistors. *Am. Ceram. Soc. Bull.*, 1993, **72**, 69–76.
4. Ting, C.-J., Peng, C.-J., Lu, H.-Y. and Wu, S.-T., Lanthanum–magnesium and lanthanum–manganese donor-acceptor-codoped semiconducting barium titanate. *J. Am. Ceram. Soc.*, 1990, **73**, 329–334.
5. Cheng, H.-F., Effect of sintering aids on the electrical properties of positive temperature coefficient of resistivity $BaTiO_3$ ceramics. *J. Appl. Phys.*, 1989, **66**, 1382–1387.
6. Ueoka, H. and Yodogawa, M., Ceramic manufacturing technology for the high performance PTC thermistor. *IEEE Trans. Manuf. Technol., MFT-3*, 1974, 77–82.
7. Illingsworth, J., Al-Allak, H. M., Brinkman, A. W. and Woods, J., The influence of Mn on the grain-boundary potential barrier characteristics of donor-doped $BaTiO_3$ ceramics. *J. Appl. Phys.*, 1990, **67**, 2088–2092.
8. Hill, D. and Tuller, H., Ceramic sensors: theory and practise. In *Ceramic Materials for Electronics*, *272*, ed. R. Buchanan. Marcel Dekker Inc., NY, 1991, p. 335.
9. N. Yasuhiro, Murate Manufacturing Co., European Patent 097482, A3, July 27, 1999.
10. Blanchart, P., Balestrieri, D., Weber, F. and Abelard, P., Influence of calcium addition on the microstructure and the electrical properties at room temperature of $BaTiO_3$ for PTC thermistors. *Silicates Indust.*, 1994, **1/2**, 47–52.
11. Kuwabara, M., Morimo, K. and Matsunaga, T., Single-grain boundaries in PTC resistors. *J. Am. Ceram. Soc.*, 1996, **79**, 997–1001.
12. Nemoto, H. and Oda, I., Direct examinations of PTC action of single grain boundaries in semiconducting $BaTiO_3$ ceramics. *J. Am. Ceram. Soc.*, 1980, **63**, 398–401.
13. Hayashi, K., Yamamoto, T. and Sakuma, T., Grain orientation dependence of the PTCR effect in niobium-doped barium titanate. *J. Am. Ceram. Soc.*, 1996, **79**, 1669–1672.
14. Hayashi, K., Yamamoto, T., Ikuhara, Y. and Sakuma, T., Formation of potential barrier related to grain-boundary character in semiconducting barium titanate. *J. Am. Ceram. Soc.*, 2000, **83**, 2684–2688.
15. Hayashi, K., Yamamoto, T., Ikuhara, Y. and Sakuma, T., Misorientation dependence of grain boundary resistivity in Nb-doped barium titanate. *Key Eng. Mater.*, 2000, **181/182**, 51–54.
16. Channel 5 diffraction pattern analysis software, HKL, Denmark, 2001.
17. Humphreys, F. J., *Vmap 8.5*. Manchester Materials Science Centre, 2001.
18. Al-Allak, H. M., Illingsworth, J., Brinkman, A. W. and Woods, J., Current–voltage characteristics of donor-doped $BaTiO_3$ semiconducting ceramics. *J. Phys. D: Appl. Phys.*, 1989, **22**, 1393–1397.
19. Alles, A. B. and Burdick, V. L., Grain boundary oxidation in PTCR barium titanate thermistors. *J. Am. Ceram. Soc.*, 1993, **76**, 401–408.
20. Seaton, J. and Leach, C., Local property measurements in PTC thermistors. *Acta Mater.*, 2003, **51**, 6027–6034.
21. Kuwabara, M., Effect of microstructure on the PTCR effect in semiconducting barium titanate ceramics. *J. Am. Ceram. Soc.*, 1981, **64**, 639–644.
22. Kolodiazhnyi, T., Petric, A. and Johari, G. P., Models of the current–voltage dependence of $BaTiO_3$ with positive temperature coefficient of resistivity. *J. Appl. Phys.*, 2001, **89**, 3939–3946.